Biochimica et Biophysica Acta, 1144 (1993) 309–324

BBABIO 43882

Light-induced proton uptake by photosynthetic reaction centers from *Rhodobacter sphaeroides* R-26.1. II. Protonation of the state $DQ_AQ_B^{2-}$

P.H. McPherson, M.Y. Okamura and G. Feher

Department of Physics, 0319, University of California at San Diego, La Jolla, CA (USA)

(Received 12 November 1992)
(Revised manuscript received 15 March 1993)

Key words: Bacterial photosynthesis; Reaction center; Proton uptake; Electron transfer; (*Rb. sphaeroides*)

Proton uptake associated with the two-electron reduction of Q_B was investigated in reaction centers (RCs) from *Rhodobacter sphaeroides* R-26.1 using pH-sensitive dyes. An uptake of two protons was observed at pH $\leq$ 7.5, consistent with the formation of the dihydroquinone Q_BH_2. At higher pH, the proton uptake decreased with an apparent pK_a of approx. 8.5, i.e., to 1.5 $H^+/2$ e^- at pH 8.5. A molecular model is presented in which the apparent pK_a is due to the protonation of either the carbonyl oxygen on Q_B or of an amino acid residue near Q_B (e.g., His-L190). Experimental evidence in favor of the protonation of the oxygen is discussed. The kinetics of the electron transfer from $Q_A^-Q_B^-$ to $Q_AQ_B^{2-}$ and the associated proton uptake were compared at several pH values and temperatures. At pH 8.5 (21.5°C) the rate constants for the proton uptake and electron transfer are the same within the precision of the measurement. At lower pH, the proton uptake rate constant is smaller than that for electron transfer. The difference between the rate constants is temperature dependent, i.e., it varies from 12 ± 4% at 21.5°C (pH 7.5) to 28 ± 4% at 4.0°C (pH 7.5). We show that the kinetics can be explained by a previously proposed model (Paddock, M.L., McPherson, P.H., Feher, G. and Okamura, M.Y. (1990) Proc. Natl. Acad. Sci. USA 87, 6803–6807) in which the uptake of two protons by doubly reduced Q_B occurs sequentially, one concomitant with and the other after electron transfer.

Introduction

The reaction center (RC) in photosynthetic bacteria is a membrane-bound protein-pigment complex that is responsible for the primary process of photosynthesis, i.e., the conversion of light into chemical energy. This process involves a light-induced charge separation between donor and acceptor molecules in the RC that is accompanied by an uptake of protons. The transport of these protons across the bacterial membrane results in the formation of a proton gradient, which provides the driving force for the conversion of ADP into ATP. The reaction center (reviewed in Refs. 1–3) consists of three polypeptide subunits, L, M, and H, and nine prosthetic groups: four bacteriochlorophyll molecules, two of which form a dimer that serves as the primary electron donor (D), two bacteriopheophytin molecules, two ubiquinone-50 molecules that serve as the primary (Q_A) and secondary (Q_B) electron acceptors and a non-heme iron Fe^{2+}. The reaction center spans the bacterial membrane with the primary electron donor D towards the periplasmic side and the quinones Q_A and Q_B towards the cytoplasmic side. All of the prosthetic groups except the secondary quinone Q_B are tightly bound to the reaction center. The loosely bound Q_B serves as a mobile electron and proton carrier between the reaction center and the other complexes involved in photosynthesis (reviewed in Refs. 4,5).

The primary photochemistry involves the transfer of an electron from the photoexcited primary electron donor D* via a bacteriopheophytin and primary acceptor quinone Q_A to the secondary acceptor quinone Q_B (reviewed in Refs. 2,3,6). The oxidized donor D^+ is reduced by an exogenous secondary electron donor, which in vivo is a cytochrome c_2. Through this process two electrons and two protons are delivered to Q_B in two sequential electron transfer steps as follows (re-

Correspondence to: G. Feher, Department of Physics, 0319 University of California at San Diego, 9500 Gilman Drive, La Jolla, CA 92093-0319 USA.

Abbreviations: D, primary donor; Q_A, primary acceptor; Q_B, secondary acceptor; RC, reaction center; cyt *c*, cytochrome *c*; DAD, diaminodurene; Q_{10}, ubiquinone-50; Q_0, ubiquinone-0; LDAO, lauryldimethylamine *N*-oxide; DOC, sodium deoxycholate.

viewed in Refs. 7,8):

$$DQ_AQ_B \xrightarrow{h\nu} D^+Q_A^-Q_B \xrightarrow[\text{donor}]{\text{red sec. ox}} DQ_AQ_B^- \quad (1a)$$

$$DQ_AQ_B^- \xrightarrow{h\nu} D^+Q_A^-Q_B^- \xrightarrow[\text{donor}]{\text{red sec. ox}} DQ_AQ_BH_2 \quad (1b)$$
$$2H^+$$

where in the bacterium the protons are taken up from the cytoplasm. The dihydroquinone Q_BH_2 is released from the RC [9,10] into the membrane where it diffuses and docks with the cytochrome bc_1 complex. Subsequent oxidation of the dihydroquinone results in the release of protons into the periplasm, which leads to the formation of the chemiosmotic gradient. The proton uptake by the RC is a crucial part of this process and is the subject this work.

In paper I of this series [11], we reported on the proton uptake associated with the one-electron reduction of the quinones Q_A and Q_B. Spectroscopic evidence [12–15] and the shape of the proton uptake curves as a function of pH [11,16–18] show that the semiquinones Q_A^- and Q_B^- are not protonated directly. The observed proton uptake (not shown in Eqn. 1a) was attributed to amino-acid residues whose pK_a values are shifted due to their interaction with the charges of Q_A^- and Q_B^-. We found the proton uptake associated with both Q_A^- and Q_B^- to be significantly smaller than 1.0 H^+/e^- and to be pH dependent. From the fit of a model to the pH dependence of the proton uptake we deduced that at least four groups of residues interact with Q_A^- and Q_B^-. Maroti and Wraight [16–18] used both dyes and a conductance technique to measure the proton uptake by Q_A^- and Q_B^- and came essentially to the same conclusions as we did, although their results differed quantitatively from ours. Recent analyses of the pH dependence of the charge recombination in mutant RCs has shown that Q_B^- has significant interactions with the protonatable residues Glu-L212 (pK_a approx. 9) [19,20], Asp-L213 ($pK_a < 7$) [20–22] and Asp-L210 ($pK_a < 7$) [23].

In this work we focus on the proton uptake associated with the transfer of the second electron to Q_B^-. Previous measurements of the proton uptake [16,18] and UV absorbance spectrum [24,25] are consistent with the uptake of two protons to form dihydroquinone. In these studies, however, the dihydroquinone observed at steady state had been released from the RC and replaced by a neutral quinone that was present in excess. These results, therefore, do not pertain to the protonation of the bound dihydroquinone. We determined the proton uptake in the absence of excess quinone thereby maximizing the amount of bound doubly-reduced Q_B. In contrast to paper I [11], we used in this work pH-sensitive dyes instead of a pH electrode to have a fast enough response time to measure the kinetics of protonation.

We obtained the pH dependence of the total steady-state proton uptake associated with the formation of doubly-reduced Q_B between pH 6 and 9. We fitted the pH dependence of the proton uptake with a phenomenological model involving the titration of a protonatable group. Whether this group is on Q_B or an amino-acid residue is discussed but not resolved.

We compared the rates of electron transfer from $Q_A^-Q_B^-$ to $Q_AQ_B^{2-}$ [a] and the associated proton uptake at several pH values and temperatures. We show that the kinetics are consistent with a model [26] that was proposed previously to explain the effects of the mutations Glu-L212 → Gln and Ser-L223 → Ala. From a fit of the model to the kinetics data, we obtained the rate constants for the two protonation steps at pH 7.5.

Materials and Methods

Reagents, buffers and dyes. Cytochrome c (cyt *c*; horse heart grade VI, Sigma) was reduced (> 99%) by hydrogen gas in the presence of platinum black (Aldrich) and purified by filtration (Schleicher and Schuell uniflo filter, 0.2 μM pore size). The concentration of cyt c^{2+} was determined from the optical absorbance and the extinction coefficient $\epsilon^{550}_{\text{cyt}\,c^{2+}} = 29.5\ \text{mM}^{-1}\ \text{cm}^{-1}$ [27]. The amount of cyt c^{2+} oxidized by RCs was quantified using the difference extinction coefficient $\varepsilon^{550}_{\text{cyt}\,c^{2+}} - \varepsilon^{550}_{\text{cyt}\,c^{3+}} = 21.1\ \text{mM}^{-1}\ \text{cm}^{-1}$ [27]. Solutions of ferrocene, diaminodurene (DAD; 2,3,5,6-tetramethyl-*p*-phenylenediamine) and ubiquinone-0 (Q_0, 2,3-dimethoxy-5-methyl-1,4-benzoquinone; purity > 99%, Aldrich) were prepared in ethanol prior to use. Ubiquinone-50 (Q_{10}, 2,3-dimethoxy-5-methyl-6-decaisoprenyl-1,4-benzoquinone, Sigma) was solubilized in 1% (w/v) LDAO (lauryldimethylamine *N*-oxide, Fluka) at 50°C and stored at −70°C. Ferrocyanide ($K_4(CN)_6$, Mallinckrodt) was prepared in water prior to use. Buffers used were: Pipes (1,4-piperazinediethanesulfonic acid, Calbiochem-Behring), pH 6.0–7.0; Hepes (*N*-2-hydroxyethylpiperazine-*N*'-2-ethanesulfonic acid, Calbiochem-Behring), pH 7.0–8.0; Tris (2-amino-2-hydroxymethylpropane-1,3-diol, Schwarz/Mann), pH 8.0–9.0; Ches (cyclohexylaminoethanesulfonic acid, Calbiochem-Behring), pH 9.0. The following pH-sensitive dyes were used at the indicated wavelengths and pH: chlorophenol red (water soluble, Aldrich), pH 6.0–7.0, $\lambda = 575$ nm; phenol red (sodium salt, Sigma), pH 7.0–8.5, $\lambda = 555$ nm; cresol red (sodium salt, Sigma), pH 8.5 $\lambda = 555$ nm.

Reaction centers. Reaction centers from *Rb.*

[a] Unless specifically noted, protonation is omitted for simplicity; e.g., $Q_AQ_B^{2-}$ represents all the protonated and unprotonated states of the RC and Q_B when Q_B is doubly-reduced.

sphaeroides R-26.1 were isolated in LDAO as described [28]. About 50% of the RCs lost their Q_B during purification (Q_A is more tightly bound and remained in the RC). The amount of Q_B per RC was increased by adding Q_{10} in 1% LDAO (after dilution, the LDAO concentration was 0.1%) followed by dialysis to reduce the LDAO concentration (48 h at 4°C against 10 mM Tris-HCl, 0.025% LDAO, 0.1 mM EDTA (pH 8)). When excess exogenous quinone (i.e., 10 Q_{10}/RC) was required, Q_{10} in LDAO was added by the same procedure. The RCs were concentrated to approx. 0.3 mM in centrifugal microconcentrators (Amicon Centricon-30) and dialized for 48 h at 4°C (against 2 mM Tris-HCl, 0.040% dodecyl-β-D-maltoside, 10 mM KCl, 0.1 mM EDTA (pH 8)) to remove LDAO, which had also been concentrated (to approx. 0.2%). The high RC and low Tris concentrations minimized the amount of Tris per RC, and, therefore, the buffer capacity. After dialysis, the total quinone content was 1.9 Q_{10}/RC (assayed by a cyt *c* photooxidation assay [29]). This included 1.0 bound Q_A/RC and 0.7–0.8 bound Q_B/RC (depending on pH; see Results for assay); the remaining 0.1–0.2 Q_{10}/RC was presumably bound non-specifically [29]. The concentration of RCs was determined from the amount of cyt c^{2+} oxidized after one laser flash (see Results); the RC extinction coefficient at 802 nm determined by this procedure was 318 ± 12 mM^{-1} cm^{-1}.

Optical absorbance measurements. Absorbance spectra were recorded on a Cary 17D spectrophotometer (Varian). Absorbance changes at a single wavelength were measured using a single-beam spectrophotometer of local design [30].

Actinic illumination. Actinic illumination was from a pulsed-dye laser (Phase R DL 2100; 0.5 μs flash width, approx. 0.2 J/flash, $\lambda_0 = 590$ nm). Light saturation of the RCs was determined to be more than 99% from the bleaching at 865 nm as a function of actinic light-intensity.

Curve fitting. Fits to data were obtained by using either the program Peakfit (Jandel) or Sigmaplot (Jandel) on an IBM compatible personal computer.

Determination of electron transfer kinetics, partition coefficients α and β, and fraction δ. The fraction δ of RCs without a bound Q_B and the partition coefficient α between the states $Q_A^- Q_B$ and $Q_A Q_B^-$ were determined optically at 865 nm from a charge recombination kinetics assay [29,30]. The partition coefficient β between the states $Q_A^- Q_B^-$ and $Q_A Q_B^{2-}$ (protonation omitted for simplicity) was obtained from the average of two assays [31], one involving the semiquinone absorbance at 450 nm and the other the cyt c^{2+} oxidation (measured at 550 nm) after a series of flashes. The rate of electron transfer $k_{AB}^{(2)}$ from $Q_A^- Q_B^-$ to $Q_A Q_B^{2-}$ was determined optically at 450 nm from the semiquinone decay.

Determination of kinetics and stoichiometry of proton uptake. Proton uptake was monitored optically using pH indicator dyes (see Reagents, buffers and dyes) in a degassed, weakly buffered solution that included 50 μM dye, 20–100 μM buffer, 0.040% (w/v) dodecyl-β-D-maltoside and 50 mM KCl. The pH was adjusted with alliquots of either 0.01 or 0.1 N NaOH and HCl. Small amounts of buffer (see Reagents, buffers and dyes) were added when necessary to keep the flash-induced pH changes less than 0.05 units. A correction for the small (< 2% of the total signal) background absorbance of the RCs was determined in a strongly buffered (10 mM) sample. The buffer capacity of this sample was at least 100-fold larger than that of the weakly buffered one in which proton uptake was measured. The change in absorbance was calibrated in terms of proton uptake (H^+/RC) by adding known amounts of HCl with a syringe (Hamilton 701; 10 μl capacity). To ensure that the change in absorbance was proportional to the number of added protons, 4–8 injections were performed with the same volume (10.0 ± 0.1 μl) but different concentrations of HCl (before injection, 0.200 mM – 1.20 mM ± 1%; diluted from a 10.00 ± 0.05 mM stock solution (Fisher)). Before each measurement, the pH was adjusted with 0.01 M KOH to the same starting value. A correction was made for the dilution of the dye caused by the additions. The estimated uncertainty in the calibration was typically ±3%.

Proton uptake was measured using 2 ml of solution contained in a thermostated quartz cuvette (1 cm path length) that was equipped with a small (3 mm diameter) glass/calomel pH electrode (Ingold # ES 18726) and a cross-shaped stirring bar (Fisher 14-511-96A). The pH electrode was calibrated with Fisher standards to an accuracy of 0.02 pH units. The stirring bar was driven by a magnetic stirrer (Troemner model 700) mounted under the cuvette holder. Mixing of added HCl was more than 99% complete in less than 5 s (with the pH electrode removed). Carbon dioxide was excluded from the cuvette by a flow of wet argon that had passed through an column of ascarite II (Aldrich) to remove CO_2. Water (quartz-double distilled) for the proton uptake solution was degassed by boiling under Argon. Care was taken that the entire volume probed by the monitoring beam of the spectrophotometer was illuminated by the laser flash. The stirring was turned off during measurement of the flash-induced absorbance changes to prevent mixing with the unilluminated part.

Theoretical models and data analysis

Stoichiometry of steady-state proton uptake

The species $DQ_A Q_B^-$ and $DQ_A Q_B^{2-}$ (protonation omitted for simplicity) are formed after one and two

laser flashes, respectively, in the presence of a secondary electron donor (cyt *c* or ferrocene) as shown in Eqns. 1a and 1b. In addition, other species are formed, since: (i) $DQ_AQ_B^-$ is in equilibrium with $DQ_A^-Q_B$ [16,30]; (ii) $DQ_AQ_B^{2-}$ is in equilibrium with $DQ_A^-Q_B^-$ [31]; and (iii) a fraction of RCs lack a bound Q_B. The mol fractions of the species present after a series of flashes is shown in Table A-I of Appendix A. The observed proton uptake has a contribution from each of these species; consequently, the proton uptakes by $DQ_AQ_B^-$ and $DQ_AQ_B^{2-}$ have to be derived from the observed values (proton uptake by residues that interact with Q_A^- and Q_B^- was omitted for simplicity from Eqns. 1a and 1b). The total observed proton uptake per RC (H^+/RC) after one and two flashes is given by Eqns. 2a and 2b, respectively:

$$\Delta H_{obs}^{+(1)} = (\chi_{Q_AQ_B^-}^{(1)})(\boldsymbol{\Delta H}_{Q_AQ_B^-}^{+}) + \sum_{i=4}^{i=6}(\chi_i^{(1)})(\Delta H_i^+) \tag{2a}$$

$$\Delta H_{obs}^{+(2)} = (\chi_{Q_B^{2-}}^{(2)})(\boldsymbol{\Delta H}_{Q_B^{2-}}^{+}) + \sum_{i=4}^{i=8}(\chi_i^{(2)})(\Delta H_i^+) \tag{2b}$$

where the superscripts (1) and (2) denote the number of flashes, the index (i) corresponds to the species number in Table A-I, χ_i is the mol fraction of species (i), and ΔH_i^+ is the proton uptake due to species (i). The proton uptakes to be determined are shown in bold face. Note that $\Delta H_{Q_B^{2-}}^+$ includes direct protonation of doubly-reduced Q_B and any proton uptake by amino-acid residues of the RC protein that interact with doubly-reduced Q_B. Rearrangement of Eqns. 2a and 2b and substitution of the expressions given in Table A-I for the mol fractions gives the following equations for the proton uptakes by $DQ_AQ_B^-$ and $DQ_AQ_B^{2-}$:

$$\boldsymbol{\Delta H}_{Q_AQ_B^-}^{+} = \frac{\Delta H_{obs}^{+(1)} - [\delta + \alpha(1-\delta)]\Delta H_{Q_A^-}^{+}}{(1-\alpha)(1-\delta)} \tag{3a}$$

$$\boldsymbol{\Delta H}_{Q_B^{2-}}^{+} = \{\Delta H_{obs}^{+(2)} - [\delta + \alpha^2(1-\delta)]\Delta H_{Q_A^-}^{+} - \alpha(1-\alpha)(1-\delta)\Delta H_{Q_AQ_B^-}^{+} - \beta(1-\alpha)(1-\delta)\Delta H_{Q_A^-Q_B^-}^{+}\}/((1-\beta)(1-\alpha)(1-\delta)) \tag{3b}$$

where the proton uptake/release by the secondary electron donor was assumed to be zero [b], δ is the fraction of RCs without a bound Q_B, α is the partition coefficient between $Q_A^-Q_B$ and $Q_AQ_B^-$, given by:

$$\alpha = \frac{[Q_A^-Q_B]}{[Q_A^-Q_B] + [Q_AQ_B^-]}, \tag{4a}$$

and β is the partition coefficient between $Q_A^-Q_B^-$ and $Q_AQ_B^{2-}$ (protonation omitted for simplicity), given by:

$$\beta = \frac{[Q_A^-Q_B^-]}{[Q_A^-Q_B^-] + [Q_AQ_B^{2-}]}. \tag{4b}$$

The values of α, β and δ were determined by standard methods (see Materials and Methods and below). The proton uptakes by DQ_A^- ($\Delta H_{Q_A^-}^+$) and $DQ_AQ_B^-$ ($\Delta H_{Q_AQ_B^-}^+$) have been determined previously [11] (We have assumed that the proton uptake is the same for DQ_A^- and $DQ_A^-Q_B$). The proton uptake by $DQ_A^-Q_B^-$ ($\Delta H_{Q_A^-Q_B^-}^+$) was approximated to be the sum of $\Delta H_{Q_A^-}^+$ and $\Delta H_{Q_AQ_B^-}^+$. Some of the doubly-reduced Q_B may be released from the RC as discussed in a later section. Eqn. 3b remains valid in this case, but gives the proton uptake associated with the total (bound and released) doubly-reduced Q_B. Note that the assays for the partition coefficient β (see below) also do not distinguish between bound and released doubly-reduced Q_B.

Determination of the partition coefficients α and β. The partition coefficient α between $Q_A^-Q_B$ and $Q_AQ_B^-$ (Eqn. 4a) was determined from the rates of charge recombination k_{AD} ($D^+Q_A^- \rightarrow DQ_A$) and k_{BD} ($D^+Q_AQ_B^- \rightarrow DQ_AQ_B$ using the relation [30]:

$$k_{BD} = \alpha \cdot k_{AD}. \tag{5}$$

Eqn. 5 holds for indirect charge recombination through Q_A as follows [30]:

$$D^+Q_AQ_B^- \rightleftharpoons D^+Q_A^-Q_B \xrightarrow{k_{AD}} DQ_AQ_B \qquad (k_{BD}) \tag{6}$$

where $D^+Q_AQ_B^-$ and $D^+Q_A^-Q_B$ are in thermal equilibrium with a fraction α of RCs in the state $D^+Q_A^-Q_B$. Kleinfeld et al. [30] showed that indirect charge recombination occurs in at least 95% of the RCs. The uncertainties given for α (see Results) are the errors that would result if direct charge recombination occurred in 5% of the RCs. The value of α was shown by Kleinfeld et al. [30] to be independent within experimental error of the redox state of the primary donor D.

The partition coefficient β (Eqn. 4b) was determined from two assays [31]. In the first, the concentration of $Q_A^-Q_B^-$ after two flashes was determined from the semiquinone absorbance at 450 nm, where neither neutral nor doubly-reduced quinone absorbs. The absorbance changes after one and two flashes (ΔA_1^{450} and ΔA_2^{450}, respectively) depend on the mol fractions and

[b] This is justified for ferrocene and ferrocyanide which were used as secondary donors in most of this work. If cyt *c* is used, the proton release ($-\Delta H_{cyt\,c^{3+}}^+$) by oxidized cyt *c* [11] must be taken into account. This requires the addition of the term $-\Delta H_{cyt\,c^{3+}}^+$ to the numerator of Eqn. 3a and the term $-[1+(1-\alpha)(1-\delta)]\Delta H_{cyt\,c^{3+}}^+$ to the numerator of Eqn. 3b ($\Delta H_{cyt\,c^{3+}}^+$ is negative).

extinction coefficients for the semiquinone states (see Table A-I). From Table A-I in Appendix A, one can derive the following expression for β (see Ref. 31 for the derivation; a small term contributing less than 0.01 to β is not included in Eqn. 7):

$$\beta = \frac{\epsilon^{450}_{Q_A Q_B^-} + \alpha\left(\epsilon^{450}_{Q_A^- Q_B} - \epsilon^{450}_{Q_A Q_B^-}\right)}{\epsilon^{450}_{Q_A^- Q_B^-}} \frac{(1-\alpha)(1-\delta)\Delta A_1^{450} + \Delta A_2^{450}}{(1-\alpha)(1-\delta)\Delta A_1^{450}} \tag{7}$$

where the extinction coefficients for the states $Q_A^- Q_B$, $Q_A Q_B^-$ and $Q_A^- Q_B^-$ were determined in Ref. 31 to be (in $mM^{-1}\ cm^{-1}$), respectively:

$$\epsilon^{450}_{Q_A^- Q_B} = 4.9 \pm 0.1, \tag{8a}$$

$$\epsilon^{450}_{Q_A Q_B^-} = 6.1 \pm 0.1, \tag{8b}$$

$$\epsilon^{450}_{Q_A^- Q_B^-} = 9.7 \pm 0.3 \tag{8c}$$

In the second assay the partition coefficient β was determined from the amount of cytochrome c oxidized (measured at 550 nm) after a series of three flashes. Since the species $DQ_A^- Q_B^-$ cannot oxidize a cyt c^{2+} after a flash (see Appendix A), the amount of cyt c^{2+} oxidized after the third flash is reduced with respect to the first flash by an amount determined by the fraction of $Q_A^- Q_B^-$ formed after the second flash. From the absorption changes one can determine β as follows (derived in Ref. 31):

$$\beta = \frac{(1-\delta)\Delta A_1^{550} - \Delta A_2^{550}}{(1-\delta)\Delta A_1^{550}} + \frac{\Delta A_2^{550} - \Delta A_3^{550}}{\Delta A_2^{550}} \tag{9}$$

where the first term corresponds to the partition coefficient α [30].

Results

Determination of the RC concentration

To determine the proton uptake, the concentration of photochemically active RCs had to be known. The concentration was determined from the amount of cyt c^{2+} oxidized by D^+ after a single saturating (> 99%) laser flash. The cyt c^{2+} oxidation was monitored optically at 550 nm (bandwidth = 1 nm) and quantified using the cytochrome c difference extinction coefficient $\epsilon^{550}_{\text{cyt } c^{2+}} - \epsilon^{550}_{\text{cyt } c^{3+}} = 21.1 \pm 0.4\ mM^{-1}\ cm^{-1}$ [27]. A small correction (approx. 3%) for the RC absorbance was determined using the electron donor DAD, which does not absorb at 550 nm. Reduction of D^+ by cyt c^{2+} was greater than 99% (measured optically at 865 nm). Measurements were made in 10 mM Hepes, 0.040% dodecyl-β-D-maltoside, 50 mM KCl (pH 7.5), $T = 21.5$°C with 2 μM RCs and 35 μM cyt c^{2+}. The RC concentration thus determined is given in terms of an observed extinction coefficient at 802 nm, which is valid for 100% active RCs:

$$\epsilon^{802}_{RC} = 318 \pm 12\ mM^{-1}\ cm^{-1} \tag{10}$$

This value is the average of seven measurements performed on different RC preparations; the experimental error was estimated from the standard deviation of the mean and the uncertainty in $\epsilon^{550}_{\text{cyt } c^{2+}} - \epsilon^{550}_{\text{cyt } c^{3+}}$. The variation of the observed ϵ^{802}_{RC} (311–323 $mM^{-1}\ cm^{-1}$) among different RC preparations was larger than the precision (1%) of the measurement. The individual value obtained for the preparation that was used to determine proton uptake was therefore used to quantify the proton uptake.

Because the method described above relies on the difference extinction coefficient $\epsilon^{550}_{\text{cyt } c^{2+}} - \epsilon^{550}_{\text{cyt } c^{3+}}$, its value was checked as follows: The difference extinction coefficient was determined from the absorbance change observed for the oxidation of a known amount of cyt c^{2+}. The cyt c^{2+} was oxidized by a known amount of Q_0 (determined by weight); 2 cyt c^{2+} were oxidized per Q_0. The reaction was catalyzed by RCs under continuous illumination (0.1 RC/Q_0) [29]. A correction (approx. 10%) for the cyt c oxidized by the RCs was determined without Q_0. The value of $\epsilon^{550}_{\text{cyt } c^{2+}} - \epsilon^{550}_{\text{cyt } c^{3+}}$ agreed with that in Ref. 27 (21.1 $mM^{-1}\ cm^{-1}$) within the experimental uncertainty of $\pm 2\%$.

The value of ϵ^{802}_{RC} shown in Eqn. 10 is in fair agreement with that reported previously by Straley et al. [32] ($\epsilon^{802}_{RC} = 288 \pm 14\ mM^{-1}\ cm^{-1}$). In contrast to the cyt c^{2+} photooxidation method, the technique used by Straley et al. (pigment extraction) is sensitive to both photochemically active and inactive RCs. Furthermore, the procedure for preparing RCs has been modified [1,28] since the publication of Ref. 32.

The partition coefficient α and fraction δ

The partition coefficient α between the states $Q_A^- Q_B$ and $Q_A Q_B^-$ (see Eqn. 4a) and the fraction δ of RCs without a bound Q_B had to be determined in order to quantify the proton uptake. They were determined from the kinetics of charge recombination measured optically at 865 nm (data not shown) and are shown in Table 1 for several pH values. The absorbance change at 865 nm is associated with the formation and decay of D^+. The decay is biphasic corresponding to the two charge recombinations $D^+ Q_A Q_B^- \rightarrow D Q_A Q_B$ ($k_{BD} \cong 1\ s^{-1}$ (pH 7.5)) and $D^+ Q_A^- \rightarrow D Q_A$ ($k_{AD} \cong 8\ s^{-1}$ (pH 7.5)) in RCs with and without a bound Q_B. The rates k_{BD} and k_{AD} and amplitudes associated with the two phases were determined by fitting the data with a double exponential (see Materials and Methods). The value of δ was determined from the relative ampli-

TABLE I

Partition coefficients α and β and fraction δ used to determine proton uptake

Partition coefficient α is defined: $\alpha = [Q_A^- Q_B]/([Q_A^- Q_B] + [Q_A Q_B^-])$; it was determined from a charge recombination kinetics assay [30] (see Eqn. 5). Experimental uncertainty is ±0.02 (discussed in theoretical models and data analysis; see Eqns. 5 and 6). Conditions: 2 μM RCs, 50 μM pH-sensitive dye (see Materials and Methods), 0.040% dodecyl-β-D-maltoside, 50 mM KCl, 21.5°C. δ is fraction of RCs without a bound Q_B; it was determined from a charge recombination kinetics assay [29] (see text). Expermimental error is ±0.02 determined from uncertainty in fit to kinetics. Conditions: same as for α. Partition coefficient β is defined by: $\beta = [Q_A^- Q_B^-]/([Q_A^- Q_B^-] + [Q_A Q_B^{2-}])$ (protonation omitted for simplicity); it was determined from the average of two assays [31] (see Eqns. 7 and 9) at pH ≧ 7.5 and from one assay (see Eqn. 9) at pH < 7.5 as discussed in text. Experimental uncertainty corresponds to half the difference in the results of the two assays and is ±0.02 unless otherwise indicated. Conditions: 2 μM RCs, 10 mM buffer (see Materials and Methods), 0.040% dodecyl-β-D-maltoside, 50 mM KCl, 21.5°C.

pH	α	δ	β
6.3	0.08	0.23	0.00
7.0	0.09	0.24	0.00
7.5	0.09	0.26	0.01
8.0	0.10	0.27	0.02
8.5	0.11	0.31	0.20
9.0	0.13	0.33	0.43±0.05

tudes of the two phases. The partition coefficient α was determined from k_{BD} and k_{AD} using Eqn. 5.

The fraction δ was sensitive to the experimental conditions; e.g., in the presence of the pH-sensitive dyes (see Materials and Methods) it was approx. 10% larger at all pH (pH 6–9) than in the absence of the dyes. Furthermore, the increase observed in δ with increased pH (see Table I) was not reversed when the pH was lowered. Therefore, care was taken to keep the conditions of the RC samples used to measure δ and the proton uptake identical. The values of α (see Table I) were not sensitive to the presence of the dyes and are in fair agreement with those determined in Ref. [30] for a different detergent (LDAO) and ionic strength (15 mM).

The partition coefficient β

A knowledge of the equilibrium partition coefficient β between the semiquinone $Q_A^- Q_B^-$ and doubly-reduced Q_B states (see Eqn. 4b) is necessary for the determination of the proton uptake. It was obtained from the average of two assays [31]. In the first, the fraction of $Q_A^- Q_B^-$ was determined from the semiquinone absorbance at 450 nm (data not shown) after two laser flashes using Eqns. 7 and 8. The secondary donor to D^+ was DAD, which does not absorb at 450 nm at pH ≧ 7.5 [24]. This assay was limited to pH ≧ 7.5 because we observed a significant absorbance change for the oxidation of DAD at pH 6.5. The partition coefficient α was obtained from Table I and δ was determined as discussed above but under the same conditions used to measure β, i.e., without a pH-sensitive dye present. The dyes were omitted because they absorb at 450 nm and would interfere with the measurement. In the second assay cyt c^{2+} was used as the electron donor to D^+. The fraction of $Q_A^- Q_B^-$ was determined from the amount of cyt c^{2+} oxidized (measured at 550 nm; data not shown) after three flashes using Eqn. 9. The average values of β thus determined (see Table I) are in qualitative agreement with those of Kleinfeld et al. [31], who observed for a different detergent (LDAO) and ionic strength (15 mM) a pH profile that is similar but shifted about 0.5 units to higher pH.

Stoichiometry of proton uptake

The states $DQ_A Q_B^-$ and $DQ_A Q_B^{2-}$ (protonation omitted for simplicity) were formed after one and two laser flashes, respectively, with ferrocene [18] present to reduce D^+. The ferrocene was re-reduced by ferrocyanide to prevent the uptake of OH^- by the oxidized ferrocene. These secondary electron donors were chosen for their lack of proton uptake/release and for not having a significant absorbance change at 550–600 nm. The rate of reduction of D^+ was 250 s^{-1} at pH 6–9 (for a ferrocene concentration of 60 μM). Proton uptake was measured optically using pH-sensitive dyes (see Materials and Methods) as shown in Fig. 1 for pH 8.5. A small correction (≦ 2% of $\Delta H_{obs}^{+(2)}$ at pH 6–9) for the absorbance change of the RCs determined in a

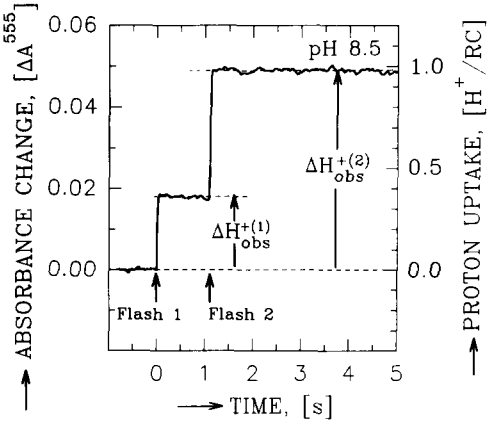

Fig. 1. Observed proton uptake, $\Delta H_{obs}^{+(2)}$, determined from the absorbance change of cresol red at 555 nm. The absorbance was calibrated in terms of H^+/RC (right ordinate) by adding a known amount of HCl. A small (2%) background absorbance (due to RCs) determined in a strongly buffered (10 mM Tris) sample was subtracted. The RC concentration was determined from the amount of cyt c^{2+} oxidized after a single laser flash using the cytochrome c extinction coefficient $\epsilon_{cyt\,c^{2+}}^{550} - \epsilon_{cyt\,c^{3+}}^{550} = 21.1\ mM^{-1}\ cm^{-1}$. The proton uptake by $DQ_A Q_B^{2-}$ (see Fig. 2) was determined from the observed value $\Delta H_{obs}^{+(2)}$. Conditions: 2 μM RCs, 60 μM ferrocene, 1 mM ferrocyanide, 50 μM cresol red, 0.040% dodecyl-β-D-maltoside, 50 mM KCl, pH 8.5, 21.5°C.

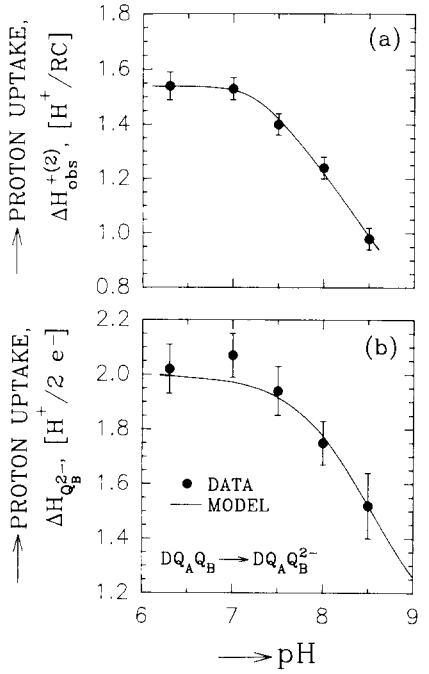

Fig. 2. Proton uptake by $DQ_AQ_B^{2-}$ in the absence of excess Q_{10}. (a) Observed proton uptake $\Delta H^{+(2)}_{obs}$ determined after two flashes as shown in Fig. 1. Error bars were estimated from the standard deviation of the mean of at least three measurements and the experimental uncertainty in the calibration of absorbance changes in terms of H^+/RC. (b) Proton uptake by $DQ_AQ_B^{2-}$ determined from $\Delta H^{+(2)}_{obs}$ using Eqn. 3b to correct for the fraction of RCs without doubly-reduced Q_B (see text). Solid line represents the titration of one protonatable group with a pK_a of 8.5. The proton uptake was 2.0 ± 0.1 $H^+/2$ e^- (pH 6–9) in the presence of excess Q_{10} which displaced the doubly-reduced Q_B into the solution (data not shown). Even in the absence of excess Q_{10}, some of the doubly-reduced Q_B may have been released from the RC (see Discussion and Conclusions). Error bars estimated from uncertainties in parameters used in Eqn. 3b. Conditions were the same as in Fig. 1, except for different pH and dyes (see Materials and Methods).

strongly buffered (10 mM Tris at pH 8.5) sample was subtracted. The absorbance change of the dye was calibrated in terms of H^+/RC (right ordinate in Fig. 1) by adding known amounts of HCl (see Materials and Methods).

The pH dependence of the total observed proton uptake $\Delta H^{+(2)}_{obs}$ after two flashes is shown in Fig. 2a. Data collection was limited to a pH range where the mol fraction of $DQ_AQ_B^{2-}$ (see Table A-I in Appendix A) was at least 0.5, i.e., pH < 9.

The proton uptake by $DQ_AQ_B^{2-}$ (Fig. 2b) was determined from $\Delta H^{+(2)}_{obs}$ and Eqn. 3b. The values of α, β and δ were obtained from Table I. The proton uptake by DQ_A^- ($\Delta H^+_{Q_A^-}$) was obtained from Fig. 5 in Ref. 11; the values are (experimental uncertainty: ± 0.02 H^+/e^-):

$$\Delta H^+_{Q_A^-} = H^+/e^- = \begin{cases} 0.30 \text{ at pH } 6.3 \\ 0.33 \text{ at pH } 7.0 \\ 0.31 \text{ at pH } 7.5 \\ 0.31 \text{ at pH } 8.0 \\ 0.38 \text{ at pH } 8.5 \end{cases} \quad (11)$$

The proton uptake by $DQ_AQ_B^-$ ($\Delta H^+_{Q_AQ_B^-}$) was obtained from $\Delta H^{+(1)}_{obs}$ (see Fig. 1; pH dependence not shown) using Eqn. 3a. The values are (experimental uncertainty: ± 0.02 H^+/e^-):

$$\Delta H^+_{Q_AQ_B^-} = H^+/e^- = \begin{cases} 0.57 \text{ at pH } 6.3 \\ 0.33 \text{ at pH } 7.0 \\ 0.31 \text{ at pH } 7.5 \\ 0.33 \text{ at pH } 8.0 \\ 0.38 \text{ at pH } 8.5 \end{cases} \quad (12)$$

The values given in Eqn. 12 are in good agreement with those determined in Ref. 11 using a pH electrode.

The proton uptake by $DQ_A^-Q_B^-$ ($\Delta H^+_{Q_A^-Q_B^-}$) was not measured directly but was approximated by taking the sum of $\Delta H^+_{Q_A^-}$ (Eqn. 11) and $\Delta H^+_{Q_AQ_B^-}$ (Eqn. 12). To check the effect of an error in this approximation, the derived proton uptake $\Delta H^+_{Q_B^{2-}}$ was also calculated for an extreme case in which $\Delta H^+_{Q_A^-Q_B^-}$ was set equal to $\Delta H^+_{Q_AQ_B^-}$; the proton uptake thus derived at pH $\leqq$ 8.0 was the same within 0.01 $H^+/2$ e^- as that in Fig. 2b (because of the small value of β) and at pH 8.5 was only 0.08 $H^+/2$ e^- larger than that in Fig. 2b. At all pH values (6.3–8.5) the dominant term in Eqn. 3b is $\Delta H^{+(2)}_{obs}$; the other terms represent a total correction varying from 6% at pH 6.3 to 23% at pH 8.5.

The proton uptake by $DQ_AQ_B^{2-}$ (Fig. 2b) is within experimental error equal to 2.0 $H^+/2$ e^- at pH $\leqq$ 7.5 but decreases at higher pH. The sold line in Fig. 2b is the fit to the data of a classical titration curve for one proton (see Eqn. 14 in Discussion); the pK_a thus determined is 8.5.

Several conditions were varied to check the method of determining proton uptake: (i) The proton uptake was determined with excess exogenous quinone present (Q_{10}; see Materials and Methods), to allow doubly-reduced Q_B to exchange with a neutral quinone from solution. The released doubly-reduced quinone should be doubly protonated, since the pK_a values for hydroquinone in aqueous solution are large (i.e., $\geqq$ 13 in 80% EtOH [33]), resulting in an uptake of two protons. The proton uptake was determined at pH 6.3, 7.5 and 8.5 to be within $\pm 2\%$ equal to 2.00 $H^+/2$ e^-. The agreement of these values with the expected uptake of two protons verifies the basic procedure for determining $\Delta H^{+(2)}_{obs}$ and the absence of any significant proton release from the secondary electron donors to D^+. (ii) The concentrations of ferrocene and ferrocyanide were varied independently at pH 8.5 from 10 to 60 μM and 1 to 10 mM, respectively. There was no effect on the observed proton uptake showing that the reduction rate of D^+ was much faster than the charge recombination. (iii) Two different dyes (phenol red and cresol red) were used at pH 8.5; the observed proton uptake was the same. Since phenol red was also used at pH 7.0–7.5 where an uptake of two protons was observed

(see Fig. 2b), the uptake of less than two protons at pH > 7.5 is unlikely to be due to some artifact associated with the dye. (iv) The time between the first and second flash was varied between 100 ms and 1.1 s to check for any decay of $DQ_AQ_B^-$ between the flashes; the observed proton uptake was the same for the two times. (v) The pH was cycled between pH 7.5 and 8.5 to check for a possible irreversible change; the proton uptake at pH 7.5 was unaffected.

Kinetics of electron transfer and proton uptake after the second flash

Electron transfer. The rate of electron transfer $k_{AB}^{(2)}$ from $Q_A^-Q_B^-$ to $Q_AQ_B^{2-}$ (protonation omitted for simplicity) was determined optically at 450 nm from the semiquinone decay after the second flash as shown for pH 7.5 in Fig. 3a. Ferrocene and ferrocyanide were used to reduce the oxidized primary donor D^+. The reduction of D^+ at the solubility limit of ferrocene (approx. 100 μM) occurs at a rate similar to $k_{AB}^{(2)}$ and would interfere with the measurement. It was made, therefore, slower (approx. 100 s^{-1} at pH 7.5) by reducing the ferrocene concentration. Consequently, the decay was biphasic with the fast phase corresponding to electron transfer $k_{AB}^{(2)}$ and the slow phase corresponding to reduction of D^+. The kinetics were fitted with a double-exponential decay (solid line in Fig 3a is slow phase). The fit to the fast phase $k_{AB}^{(2)}$ is shown in Fig. 3b (solid line) on an expanded time scale with the slow phase subtracted. The rate $k_{AB}^{(2)}$ determined at several pH values and temperatures is shown in Table II. The values at 21.5°C agree within 30% with those determined previously by Kleinfeld et al. [31] for a different detergent (LDAO) and ionic strength (15 mM).

Proton uptake. The kinetics of proton uptake were determined under the same conditions used for the electron transfer $k_{AB}^{(2)}$, except for the addition of a pH indicator dye. The absorbance change of the dye (phenol red at pH 7.5) after the second flash is shown in Fig. 4a with the absorbance change of a strongly buffered sample (10 mM Hepes at pH 7.5) subtracted. The kinetics were fitted with a double-exponential rise. The slow, minority, phase (solid line) corresponds to the reduction of D^+ and is due to an uptake of protons by amino-acid residues whose pK values are shifted through interactions with D^+ [11,17,18]. The fast, majority, phase is the proton uptake associated with the electron transfer from $Q_A^-Q_B^-$ to $Q_AQ_B^{2-}$ and is shown in Fig. 4b (solid line corresponds to exponential fit) on an expanded time scale with the slow phase subtracted. The fitted rate constants $k_{H_{obs}^{(2)}}$ at several pH values and temperatures are shown in Table II. The electron transfer $k_{AB}^{(2)}$ and proton uptake $k_{H_{obs}^{(2)}}$ rate constants are the same within the precision of the measurement at pH 8.5 and 21.5°C, but differ slightly at lower pH. This difference was investigated as a function of temperature at pH 7.5 (see Table II). At 4.0°C, the rate constant $k_{AB}^{(2)}$ is about 30% larger than $k_{H_{obs}^{(2)}}$. In order to insure that the dye could respond fast enough at pH 7.5, we measured the rate of a known fast proton uptake: that by $D^+Q_A^-$. The observed rate at 21.5°C, 7500 ± 800 s^{-1}, is in agreement with that reported previously [34] and is approx. 5-times larger than $k_{AB}^{(2)}$. The rate at 4.0°C, 3400 ± 200, is approx. 4-times larger than $k_{AB}^{(2)}$. Therefore, the difference between $k_{H_{obs}^{(2)}}$ and $k_{AB}^{(2)}$ at pH 7.5 is not due to a slow dye response. To

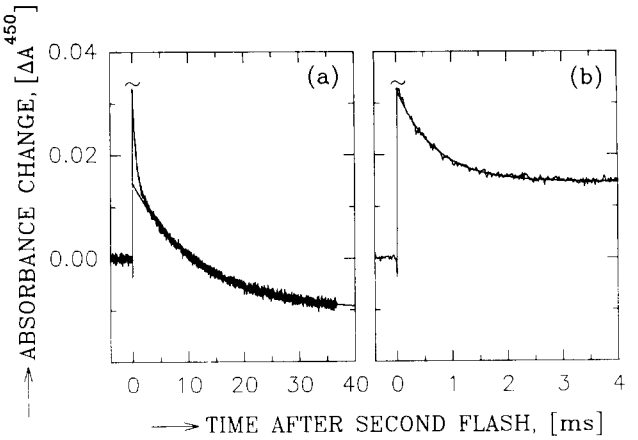

Fig. 3. Determination of the kinetics of electron transfer $k_{AB}^{(2)}$ from $Q_A^-Q_B^-$ to $Q_AQ_B^{2-}$. (a). Absorbance change at 450 nm after second flash. The rapid rise in absorbance at $t = 0$ is due to the formation of $D^+Q_A^-Q_B^-$ from $DQ_AQ_B^-$ (an artifact due to the laser flash has been truncated). The fast decay corresponds to electron transfer $k_{AB}^{(2)}$ from $D^+Q_A^-Q_B^-$ to $D^+Q_AQ_B^{2-}$ and the slow decay to the reduction of D^+ by ferrocene (fitted with single exponential, solid line). (b). Data from (a) replotted on an expanded time scale with the slow decay subtracted. Rate constant $k_{AB}^{(2)}$ (Table II) was determined from the fit of a single exponential (solid line) to the data. Conditions: 2 μM RCs, 20 μM ferrocene, 1 mM ferrocyanide, 0.040% dodecyl-β-D-maltoside, 50 mM KCl, pH 7.5, 21.5°C.

TABLE II

Kinetics of electron transfer $k_{AB}^{(2)}$ and proton uptake $k_{H_{obs}^{(2)}}$ ($Q_A^-Q_B^- + 2H^+ \rightarrow Q_AQ_BH_2$)

Experimental uncertainties are S.D. of the mean of at least four measurements. Observed rate $k_{AB}^{(2)}$ of electron transfer from $Q_A^-Q_B^-$ to Q_B^{2-} determined from fit of single exponential to decay of semiquinone absorbance at 450 nm (see e.g., Fig. 3b). The values are equilibrium rates, i.e., they are the sum of the forward and reverse electron transfer rates. At pH $\leq$ 7.5, where the partition coefficient β is small (see Table I), the equilibrium and forward electron transfer rates are essentially the same. Observed rate $k_{H_{obs}^{(2)}}$ of proton uptake associated with electron transfer from $Q_A^-Q_B^-$ to Q_B^{2-} determined from fit of single exponential to absorbance change of pH-sensitive dye (see e.g., Fig. 4b).

pH	T (°C)	rate (s^{-1})	
		$k_{AB}^{(2)}$	$k_{H_{obs}^{(2)}}$
6.3	21.5	6000 ± 150	5450 ± 200
7.5	21.5	1460 ± 50	1300 ± 15
7.5	4.0	880 ± 30	690 ± 10
8.5	21.5	435 ± 10	415 ± 15

test whether the presence of phenol red affected the rate of protonation of Q_B^{2-}, we reduced the concentration of the dye from 50 μM to 10 μM; there was no effect, within experimental error, on $k_{H^{(2)}_{obs}}$.

Effect of deoxycholate on electron and proton transfer rates

The detergent sodium deoxycholate (DOC) is often used to solubilize Q_{10} prior to addition to RCs. RCs that were reconstituted with Q_{10} in 10% (w/v) DOC exhibited electron transfer rates $k_{AB}^{(2)}$ up to 5-times faster (pH 7.5) than RCs reconstituted with Q_{10} in LDAO, even after extensive (48 h) dialysis against a sufficient volume of buffer to reduce the DOC content to less than 0.1 DOC/RC (RCs in Table II had Q_{10} added in LDAO). The proton uptake rates $k_{H^{(2)}_{obs}}$ were up to 3-times faster. The increase in $k_{AB}^{(2)}$ was also observed after addition of DOC (without Q_{10}) directly to the RC sample; the rate was increased by a factor of 3 at a DOC concentration of 0.1% (w/v) (the effect on proton uptake was not measured). The increase in the rate could be completely reversed by washing the RCs on a DEAE column with buffer (15 mM Tris, 0.1% LDAO, 1 mM EDTA), followed by elution with a 0–250 mM NaCl gradient. Two peaks eluted (at approx. 50 and approx. 100 mM NaCl). The ratio A_{280}/A_{802} of the RCs in the two peaks was the same indicating the same purity. The rate $k_{AB}^{(2)}$ for the RCs in the first peak was within experimental error ($\pm$5%) the same as the value before addition of Q_{10} in DOC; the rate was 20% larger for the RCs from the second peak. These results indicate that DOC is not completely removed by extensive dialysis (2 days) but can be removed by washing on a column. Since DOC is negatively charged, RCs with bound DOC would require a higher salt concentration for elution from the positively charged DEAE column. The RCs in the second elution peak exhibiting a larger $k_{AB}^{(2)}$ may have contained, therefore, some bound DOC.

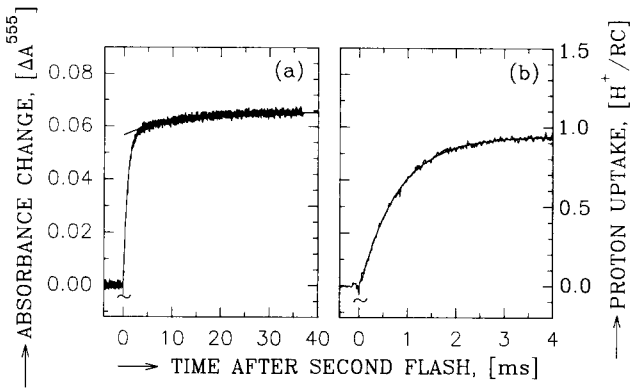

Fig. 4. Determination of proton uptake kinetics after the second flash. (a) Absorbance change of phenol red. A background absorbance change (due to RCs) determined in a strongly buffered (10 mM Hepes) sample was subtracted (an artifact due to the laser flash has been truncated). The absorbance change was calibrated in terms of H^+/RC (right, ordinate) by adding a known amount of HCl. Fast phase is the proton uptake associated with the reaction $D^+Q_A^-Q_B^- \rightarrow D^+Q_AQ_B^{2-}$. Slow phase (solid line is single-exponential fit) is associated with the reduction of D^+ by ferrocene and is due to shifts in the pK_a values of amino-acid groups that interact with D^+. (b). Data of (a) plotted on an expanded time scale with the slow phase subtracted. The observed proton uptake rate constant $k_{H^{(2)}_{obs}}$ (Table II) was determined from the fit of a single exponential (solid line). Conditions: 2 μM RCs, 20 μM ferrocene, 1 mM ferrocyanide, 50 μM phenol red, 0.040% dodecyl-β-D-maltoside, 50 mM KCl, pH 7.5, 21.5°C.

Discussion and Conclusions

Stoichiometry of proton uptake by doubly-reduced Q_B

We have measured proton uptake associated with the formation of doubly-reduced Q_B between pH 6 and 9 using pH-sensitive dyes. The total proton uptake at pH $\leqq$ 7.5 was equal to 2.0 $\pm$ 0.1 $H^+/2\ e^-$. Above pH 7.5 proton uptake decreased, i.e., to 1.52 $\pm$ 0.12 $H^+/2\ e^-$ at pH 8.5. This is smaller than the value of 2.0 expected for the formation of dihydroquinone Q_BH_2. When excess exogenous Q_{10} was present, an uptake of 2.0 $H^+/2\ e^-$ was observed at all pH (6–9) consistent with the formation of dihydroquinone. This latter measurement was a test of the,protonation of free doubly-reduced quinone, since neutral quinone that is present in excess displaces doubly-reduced Q_B. The uptake of less than two protons at pH > 7.5 occurs only when doubly-reduced Q_B is not replaced in the Q_B pocket with a neutral quinone.

Previous direct measurements [16,18] of proton uptake were done with excess quinone present and did not indicate, therefore, an uptake of less than two protons at pH > 7.5. Similarly, the reported UV absorbance spectrum, which is indicative of a dihydroquinone [24,25], was also determined in the presence of excess quinone. In the one study [31] done without excess quinone the protonation was determined indirectly from thermodynamic relations between various redox states of Q_A and Q_B. A total uptake of two protons at pH < 10 was deduced, one after the formation of $DQ_AQ_B^-$ [30] and another after the subsequent formation of $DQ_AQ_B^{2-}$ [31]. However, as discussed in Ref.11 (see also Eqn. 12) the proton uptake by $DQ_AQ_B^-$ is significantly less than 1.0 H^+/e^-, making the model in Ref. 31 incorrect. This, however, does not affect any of the other conclusions in Ref. 31.

The interpretation of our results depends on whether or not doubly-reduced Q_B remained bound. This question merits, therefore, further discussion. Binding of doubly-reduced Q_B was maximized by using a low detergent concentration (0.04% maltoside) and omitting excess exogenous neutral quinone, which, if present, would displace bound Q_BH_2 [10]. The amount of

bound doubly-reduced Q_B cannot, however, be quantified from the available experimental data. Furthermore, there is scant published work that pertains to this problem. Diner et al. [35] studied the binding of radioactively labeled quinol and quinone to RCs and concluded that the quinol was probably more loosely bound than the quinone. Okamura et al. [36] found that reducing conditions (i.e., formation of Q_BH_2) facilitated the removal of Q_B from the RC, suggesting that quinol is more loosely bound than quinone. Both of these studies were done with a high concentration of detergent (approx. 1% LDAO), which resulted in weak binding of both the quinone and quinol. Furthermore, in these studies neither a binding constant for the quinone and quinol nor the pH dependence of binding was determined. Therefore, neither study provides the information necessary to quantify the amount of bound doubly-reduced Q_B. Another study involving quinol binding was done by McPherson et al. [10], who investigated the reaction consisting of the following three sequential steps: (i) release of Q_BH_2, (ii) binding of a neutral quinone (present in excess) to the Q_B site and (iii) reduction of Q_B to a semiquinone. The observation of step (iii) was used as evidence that the precurser steps (i) and (ii) had occurred. These results do not indicate, however, whether step (i) is energetically favorable, since steps (ii) and/or (iii) could provide the driving force for the overall reaction. Therefore, further work is required to determine whether doubly-reduced Q_B is bound or released in the absence of excess quinone at a low concentration of detergent.

The uptake of less than two protons at pH > 7.5 requires two different explanations depending on whether doubly-reduced Q_B is bound or released (in the absence of excess quinone). They are: (i) If doubly-reduced Q_B is released, the released quinol should be fully protonated. The uptake of less than two protons at pH > 7.5 could be due to a release of protons from an amino-acid residue (or residues) whose pK_a value is shifted when the Q_B site becomes unoccupied. This explanation can, in principle, be tested by measuring the proton uptake associated with quinone binding to the Q_B site, e.g., after injection of quinone into a solution containing Q_B-depleted RCs. The residues that might be involved in proton release are the same as those discussed below for the second case. (ii) If doubly-reduced Q_B remains bound, the smaller proton uptake at pH > 7.5 could be associated either with a pK_a of the carbonyl oxygen of Q_B or of a residue that interacts with Q_BH_2 and releases protons. As discussed below, there is some experimental evidence in favor of the carbonyl oxygen. We shall discuss, therefore, this case in more detail.

We modeled the pH dependence of proton uptake phenomenologically with the following simple scheme:

$$Q_B + 2e^- \xrightarrow{H^+} (Q_BH)^- \underset{pK_a}{\overset{H^+}{\rightleftharpoons}} Q_BH_2 \qquad (13)$$

The proton uptake is given by:

$$\Delta H^+_{Q_B^{2-}} = 1 + \frac{1}{1 + 10^{pH - pK_a}} \qquad (14)$$

and varies from 2.0 ($pH \ll pK_a$) to 1.0 ($pH \gg pK_a$). The value of pK_a determined from a fit of Eqn. 14 to the data (Fig. 2b) is:

$$pK_a = 8.5 \pm 0.3. \qquad (15)$$

In Eqn. 14 we have neglected interactions between the charges of $(Q_BH)^-$ and protonatable residues of the RC protein. These interactions can have two effects: (i) Residues whose pK_a values are shifted due to interactions with $(Q_BH)^-$ will take up protons. If these pK_a shifts are at least as large as those for Q_B^- [11], this additional proton uptake will be significantly larger at pH > 8.5 than at pH 6.5–8.5. (ii) The pK_a of Q_BH_2 will depend on pH due to the titration of protonatable residues, which will result in an increase of negative charge (or loss of positive charge) in the vicinity of Q_B. This will destabilize $(Q_BH)^-$ relative to Q_BH_2 and will, therefore, increase the pK_a of Q_BH_2. Consequently, both (i) and (ii) would cause the proton uptake at pH > 8.5 to be larger than predicted by Eqns. 14 and 15.

Molecular model for the proton uptake by doubly-reduced Q_B

A model to explain the apparent pK_a of approx. 8.5 observed for the proton uptake by doubly-reduced Q_B is shown in Fig. 5. In this model we have assumed that the doubly-reduced Q_B remains bound. The upper panel (Fig. 5a) shows Q_B and several nearby protonatable residues. The lower panel (Fig. 5b) shows several reactions that could be important to the steady-state protonation of doubly-reduced Q_B. The apparent pK_a of approx. 8.5 observed for the proton uptake by bound doubly-reduced Q_B could be due to either titration of Q_BH_2 (reaction 2) or titration of a nearby residue that interacts with Q_BH_2 (reactions 3 and 4). Reactions 1 and 2 correspond to a model proposed in Ref. 26 that was based on results derived from mutant RCs. The proton uptake occurs via a chain of protonatable residues, which is not shown in Fig. 5b because the residues do not take up or release protons at steady state. Reactions 3 and 4 represent an alternate scheme involving a net steady-state deprotonation of a residue R that interacts with doubly-reduced Q_B. We

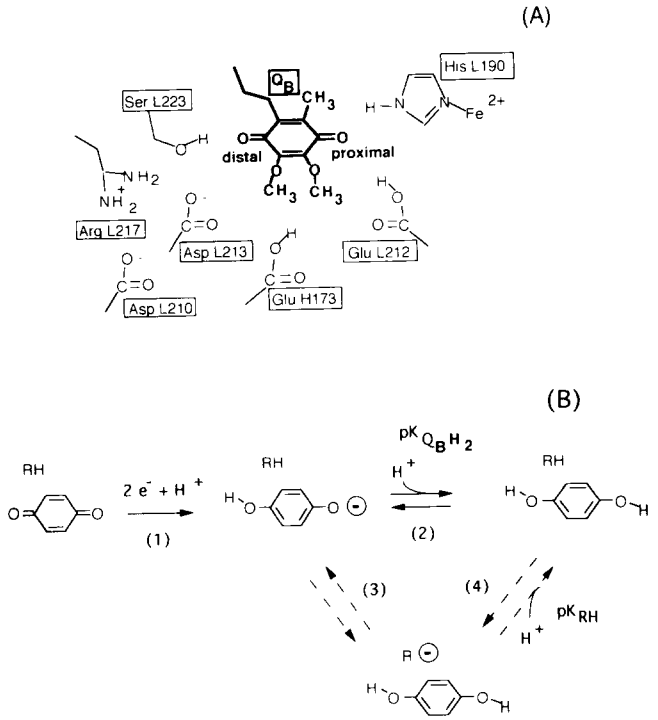

Fig. 5. Protonatable amino-acid residues in the vicinity of Q_B (A) and molecular model for the protonation of doubly-reduced Q_B (B) (for simplicity, the isoprenoid chain of Q_B has been truncated in (A) and omitted along with the methoxy and methyl groups in (B)). The distal oxygen of doubly-reduced Q_B is protonated at all pH as shown from site-specific mutagenesis of Ser-L223 [26]. The apparent pK_a of approx. 8.5 observed for proton uptake by Q_B^{2-} is due to titration of either the proximal oxygen of Q_BH_2 (reaction 2 in (B)),or to titration of a nearby amino-acid residue R (reaction 4 in (B)) whose pK_a is lowered from $pK_a \gg 8.5$ when Q_B is neutral to approx. 8.5 when Q_B is doubly-reduced to Q_BH_2. Experimental evidence (see text) supports reaction (2), i.e., $pK_a = pK_{Q_BH_2} \cong 8.5$.

shall discuss each reaction shown in Fig. 5b and present experimental evidence that supports the scheme corresponding to reaction 2.

In reaction 1 shown in Fig. 5b, two electrons and one proton are transferred to Q_B after two flashes. The proton is taken up at all pH values and binds to the distal oxygen of Q_B (near Ser-L223). This follows from results obtained on the mutants Ser-L223 → Ala [26] and Asp-L213 → Asn [21,37], which indicate that the distal oxygen must be protonated for electron transfer to Q_B^- to occur. The proximal oxygen near His-L190, however, does not need to be protonated (from solution) for electron transfer to Q_B^-. Evidence for this was obtained from mutant RCs in which Glu-L212 was replaced by Gln [19,20,38]. In this mutant the uptake of one proton (presumably by the proximal oxygen which is near Glu-L212) was slowed significantly without an effect on the rate of electron transfer to Q_B^-. Spectroscopic evidence [39] from the Glu-L212 → Gln mutant RCs also suggests that electron transfer occurs without protonation of one of the oxygens (presumably the proximal one). Therefore, the proximal oxygen is a good candidate for the group that titrates with pK_a of approx. 8.5.

The case in which the observed pK_a of approx. 8.5 is due to protonation of the proximal oxygen corresponds to reaction 2 in Fig. 5b; i.e., $pK_{Q_BH_2} \cong 8.5$. In this case R remains protonated at all pH values and is not involved. The pK_a for the titration of one proton from dihydroquinone QH_2 in aqueous solvent (80% EtOH) is approx. 13 [33], which is larger than the value of 8.5 observed in RCs. However, pK_a values in proteins can be significantly different from those in solution. The pK_a of Q_BH_2 could be lowered in the RC due to several factors: (i) Hydrogen bonding; the species $(Q_BH)^-$ could be stabilized by a hydrogen bond from His-L190 to the unprotonated proximal oxygen. (ii) Electrostatic fields; the semiquinone Q_B^- is stabilized relative to Q_A^- [16,30] and semiquinone in aqueous solvents [33]. This has been proposed to be due in part to the electrostatic field produced by nearby positive charges, e.g., the Fe^{2+} [40]. This field would also stabilize the singly protonated species $(Q_BH)^-$. (iii) Steric effects; if His-L190 is hydrogen bonded to $(Q_BH)^-$, the addition of a proton to the proximal oxygen of Q_B will be difficult without some movement of the quinone or His-L190. This movement might be energetically unfavorable, leading to a lower pK_a.

The scheme corresponding to reaction 2 in Fig. 5b is supported by experimental evidence obtained from Glu-L212 → Gln mutant RCs [c]. In this mutant, the uptake of the first proton (reaction 1) is approx. 1000-times faster than the uptake of the second proton, allowing the individual protonation steps to be resolved and analyzed. Two results are of particular importance; they are: (i) the UV difference spectrum at pH 6.5 associated with the slow uptake of the second proton resembles that expected for the protonation of $(Q_BH)^-$ to Q_BH_2 [39]. The UV difference spectrum suggests, therefore, that the state prior to the slow step (either reaction 2 or 3) is $(Q_BH)^-$. (ii) The free energy change associated with the slow proton uptake step was found from the partition coefficient β to be $\gtrsim 0$ at pH $\gtrsim 9$ (i.e., $\Delta G^0 \gtrsim 0 \pm 20$ meV at pH 9.0 and $\Delta G^0 \gtrsim +30 \pm 20$ meV at pH 9.5 (McPherson, P.H., Okamura, M.Y. and Feher, G., data not shown). Results (i) and (ii) combined imply that the energy of the state $(Q_BH)^-$ at pH > 9 is lower than or equal to that of either of the doubly protonated Q_BH_2 states shown in Fig. 5b. Consequently, $pK_{Q_BH_2} < 9$. The simplest model consistent with (i) and (ii) is that $pK_a = pK_{Q_BH_2} \cong 8.5$.

Alternate schemes involving reactions 3 and 4 in Fig. 5b cannot, however, be completely ruled out and

[c] We assume that the pK_a is similar in native and mutant RCs. This is justified because the proton uptake by the mutant at pH 8.5 is 1.5 ± 0.1 H^+/Q_B^{2-}, which is the same as that by the native RCs (McPherson, P.H., Okamura, M.Y. and Feher, G., data not shown).

merit, therefore, further discussion. In these schemes the observed pK_a of 8.5 is due either to protonation of a residue R, i.e., $pK_{RH} \cong 8.5$, or to protonation of both R and $(Q_BH)^-$, i.e., $pK_{RH} \cong pK_{Q_BH_2} \cong 8.5$. If one of these schemes is correct, which residue (or residues) interacts with doubly-reduced Q_B? One likely candidate is His-L190, which is hydrogen bonded to the proximal oxygen of neutral Q_B and ligated to the Fe^{2+} (see Fig. 5a). Since this hydrogen bond would be disrupted when Q_BH_2 is formed, the protonated species of His-L190 could be destabilized, resulting in a shift to a lower pK_a value. The pK_a value of imidazole ligated to a divalent metal (Co^{2+}) in water has been determined to be 10.0 [41], which is close to the pK_a of approx. 8.5 observed for the proton uptake. The role of His-L190 can, in principle, be tested by mutating it to a non-protonatable group. However, in RCs having a mutation at this site, the Q_B binding was found to be too weak for an accurate determination of proton uptake (Williams, J.A., Paddock, M.L., Okamura, M.Y., Feher, G., and Allen, J.P, data not shown). A second residue near Q_B is Glu-L212, which has a pK_a of approx. 9.5 [19] (when Q_B is neutral). However, deprotonation of Glu-L212 is not responsible for the observed decrease in proton uptake at pH > 7.5, since the replacement of Glu-L212 with Gln did not increase the total proton uptake, which was found to be 1.5 ± 0.1 H^+/Q_B^{2-} at pH 8.5 in the mutant (McPherson, P.H., Okamura, M.Y. and Feher, G., data not shown). Two other residues in the vicinity of Q_B, Asp-L210 and Asp-L213, have pK_a values less than 6 [20–23], and are, therefore, not involved. Two other groups shown in Fig. 5a are Arg-L217 and Glu-H173. Measurement of proton uptake by Q_B^{2-} in RCs with mutations at these sites should help to determine their role.

The details of the proposed model can be clarified by a combination of spectroscopy and proton uptake measurements on native and mutant RCs. The singly-protonated species $(Q_BH)^-$ can, in principle, be observed in the UV at approx. 310 nm [33]. However, semiquinones formed in the RC (see Table A-I) also absorb in this region and might interfere with the detection of $(Q_BH)^-$. A technique that may be more useful to test the model is Fourier Transform Infrared (FTIR) spectroscopy. FTIR is sensitive to the protonation of doubly-reduced Q_B [42] and could be used to look for the presence of the singly-protonated species $(Q_BH)^-$. FTIR has been successfully used to study protonation of residues in bacteriorhodopsin (see e.g., Ref. 43) and could be applied to look for the deprotonation of a residue after formation of doubly-reduced Q_B.

Kinetics of electron transfer and proton uptake

To understand the mechanism of electron and proton transfer to form doubly-reduced Q_B, it is important to determine the rates of these processes. The kinetics of electron transfer from $Q_A^-Q_B^-$ to Q_B^{2-} and the accompanying proton uptake were investigated at several temperatures and pH values between 6.0 and 8.5 (see Table II). The kinetics could be fitted well with single exponentials. The pH dependence of the observed electron transfer rate $k_{AB}^{(2)}$ from $Q_A^-Q_B^-$ to Q_B^{2-} was in qualitative agreement with previous results [31]. At pH 8.5 and 21.5°C the electron transfer $k_{AB}^{(2)}$ and proton uptake $k_{H^+_{obs}(2)}$ rates were the same within the precision of the measurement. At pH 7.5 and 21.5°C, $k_{AB}^{(2)}$ was $12 \pm 4\%$ larger than $k_{H^+_{obs}(2)}$. This difference in rate constants increased at lower temperature, e.g., at 4.0°C and pH 7.5, $k_{AB}^{(2)}$ was $28 \pm 4\%$ larger than $k_{H^+_{obs}(2)}$. The difference in rate constants at pH 7.5 and 21.5°C was unaffected by the presence of excess quinone. This shows that the difference is not associated with quinol/quinone exchange. A difference in rate constants was also observed by Maroti and Wraight [25] who found $k_{AB}^{(2)}$ to be about 30% larger than $k_{H^+_{obs}(2)}$ at pH 7.5 and room temperature.

The difference between the proton uptake and electron transfer kinetics can be understood in terms of a model that was proposed previously to explain results from mutant RCs [26]; it is represented by Eqn. 16:

$$\text{After two flashes: } Q_A^-Q_B^- \xrightarrow[k_{AB}^{(2)}]{H^+(1)} Q_A(Q_BH)^- \xrightarrow[k_{H^+(2)}]{H^+(2)} Q_AQ_BH_2 \tag{16}$$

The back reactions have been neglected for simplicity (for justification, see Appendix B). The key feature of this model is the sequential uptake of the two protons. The uptake of the first proton $H^+(1)$ (by the distal oxygen of Q_B; see Fig. 5) is necessary for and concomitant with the transfer of the second electron to Q_B^- at a rate $k_{AB}^{(2)}$ [26]. The temporal order of the electron and proton transfer in this first step is not known. The uptake of the second proton $H^+(2)$ (to the proximal oxygen of Q_B) at a rate $k_{H^+(2)}$ occurs after electron transfer [19,26,38].

The time dependence of the total proton uptake for the scheme in Eqn. 16 is derived in Appendix B and is given by [d]:

$$H^+/RC(t) = 2 - \left(2 + \frac{k_{AB}^{(2)}}{(k_{H^+(2)} - k_{AB}^{(2)})}\right) e^{(-k_{AB}^{(2)} \cdot t)} + \frac{k_{AB}^{(2)}}{(k_{H^+(2)} - k_{AB}^{(2)})} e^{(-k_{H^+(2)} \cdot t)}. \tag{17}$$

[d] We assume in this model that the response time of the pH indicator dye does not affect the observed rates. In Results, we showed that the response time of the dye is at least 5-fold faster than $1/k_{AB}^{(2)}$.

As an example we shall focus on the kinetics at pH 7.5. Eqn. 17 is plotted in Fig. 6 for different values of the ratio $k_{H^+(2)}/k_{AB}^{(2)}$ with $k_{AB}^{(2)}$ fixed at the measured value of 1460 s^{-1} (pH 7.5, 21.5°C). In the limit $k_{H^+(2)}/k_{AB}^{(2)} \gg 1$ (upper curve of Fig. 6), Eqn. 17 is a single exponential with a characteristic time constant equal to $1/k_{AB}^{(2)}$, i.e.:

$$H^+/RC(t) = 2(1 - e^{(-k_{AB}^{(2)} \cdot t)})$$

$$(\text{for } k_{H^+(2)}/k_{AB}^{(2)} \gg 1) \qquad (18)$$

Close to the limiting case given by Eqn. 18, the kinetics appear essentially monophasic but with a characteristic rise time that is longer than $1/k_{AB}^{(2)}$. This corresponds to the situation observed in RCs at pH 7.5. For $k_{H^+(2)}/k_{AB}^{(2)} \ll 1$, Eqn. 17 is the sum of two exponentials:

$$H^+/RC(t) = (1 - e^{(-k_{AB}^{(2)} \cdot t)}) + (1 - e^{(-k_{H^+(2)} \cdot t)})$$

$$(\text{for } k_{H^+(2)}/k_{AB}^{(2)} \ll 1) \qquad (19)$$

resulting in biphasic kinetics (see lower curves in Fig. 6).

Eqn. 17 was fitted to the data of Fig. 4b (pH 7.5, 21.5°C) with $k_{AB}^{(2)}$ fixed at the measured value of 1460 s^{-1} (see Table II) and $k_{H^+(2)}$ and the total proton uptake amplitude allowed to vary to obtain the best fit [e] (see solid line in Fig. 7). The fitted value of $k_{H^+(2)}$ was 3800 s^{-1}, i.e., about 3-times larger than $k_{AB}^{(2)}$. These results should, however, be taken as qualitative, since the accuracy of the fit is low for a ratio

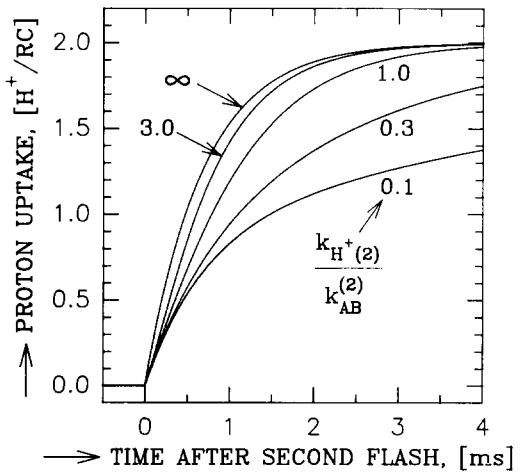

Fig. 6. Simulation of the observed proton uptake kinetics after the second flash at pH 7.5 for a simple two-step model (see Eqn. 16) in which the two protons are taken up sequentially. The first proton is taken up concomitant with electron transfer at a rate $k_{AB}^{(2)}$. The second proton is taken up at a rate $k_{H^+(2)}$ after electron transfer. Curves were computed from Eqn. 17 for different values of the ratio of rates as indicated ($k_{AB}^{(2)} = 1460$ s^{-1} (Table II) for all curves). The upper curve for the limit $k_{H^+(2)}/k_{AB}^{(2)} \gg 1$ corresponds to a single exponential with rate constant $k_{AB}^{(2)}$. The best fit of Eqn. 17 to the observed proton uptake at pH 7.5 and 21.5°C (see Fig. 7) was obtained for a ratio $k_{H^+(2)}/k_{AB}^{(2)} = 2.6$.

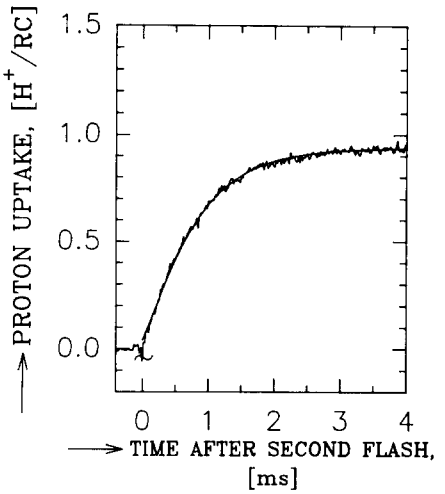

Fig. 7. Fit of two-step model (Eqn. 17; solid line) to proton uptake after second flash (proton uptake data were obtained from Fig. 4b; artifact due to laser flash has been truncated). The value of $k_{AB}^{(2)}$ was fixed at 1460 s^{-1} (see Table II) and $k_{H^+(2)}$ and the total amplitude were varied to obtain the best fit. The value of $k_{H^+(2)}$ was found to be 3800 s^{-1}.

$k_{H^+(2)}/k_{AB}^{(2)} > 1$ and several approximations were made to derive Eqn. 17 (see Appendix B). The proton uptake at 4.0°C was not fitted because the approximations have not been tested at 4.0°C. However, if Eqn. 17 is valid, the decrease in the ratio $k_{H^+(2)_{obs}}/k_{AB}^{(2)}$ with decreasing temperature (see Table II) is due to a decrease in the ratio $k_{H^+(2)}/k_{AB}^{(2)}$.

The above results show that: (i) The characteristic rise time $1/k_{H^+(2)_{obs}}$ of proton uptake is slower at pH $\leqq$ 7.5 than the electron transfer time $1/k_{AB}^{(2)}$. (ii) This difference in rise times is consistent with the sequential uptake of the two protons. (iii) For a sequential uptake, the rise time of proton uptake will be slower than $1/k_{AB}^{(2)}$, even though the first proton uptake occurs at the same rate as $k_{AB}^{(2)}$ and the second proton uptake is faster. (iv) The temperature dependence of the kinetics is consistent with the rate of uptake of the second proton being more temperature dependent than that of the first.

The scheme shown in Eqn. 16 provides a working model that can, in principle, be tested spectroscopically (e.g., by infrared absorption spectroscopy) by looking for a transient population of the state $Q_A(Q_BH)^-$. The mol fraction of the state $Q_A(Q_BH)^-$ can be determined from $k_{AB}^{(2)}$ and $k_{H^+(2)}$ using Eqn. B-2b in Appendix B. For the values of $k_{AB}^{(2)}$ and $k_{H^+(2)}$ determined at pH 7.5 and 21.5°C, the maximum predicted mol fraction is 0.2 and should occur at about 0.4 ms after the second flash. A larger maximum mol fraction is predicted at lower temperature. An alternate model, however, is possible in which doubly-reduced Q_B is

[e] The conditions for which Eqn. 17 can be scaled to fit the data are discussed in Appendix B. They are satisfied at pH 7.5 and 21.5°C.

protonated rapidly (faster than $1/k_{H^+(2)}$) by protonatable groups on the RC, which then reequilibrate more slowly with the protons and pH-sensitive dye in solution. In this case, a much smaller transient population of $Q_A(Q_BH)^-$ would be formed. Maroti and Wraight [25] have suggested this alternate model based on a comparison of rates of proton uptake, electron transfer, and dihydroquinone formation. A combination of site-specific mutations of residues that might be involved together with time-resolved spectroscopy to detect protonation states should clarify the details of the proton uptake kinetics.

Acknowledgements

We thank Ed Abresch for purifying the RCs and Mordechay Schönfeld for helpful discussions and technical assistance. The work was supported by the National Science Foundation (DMB89-15631) and National Institutes of Health (GM13191).

Appendix A

Distribution of reaction center states after successive flashes

We used Eqns. 3a and 3b in the text to determine proton uptake. These equations were derived using the expressions in Table A-I for the mol fractions of RC states after two flashes. The table is based on the following: (i) Q_A can accept only one electron. Therefore, RCs with Q_A reduced do not accept another electron from cyt c^{2+} (or ferrocene) after a flash. The reason for this is that the charge recombination $D^+I^-Q_A^- \rightarrow DIQ_A^-$ (I is the intermediate acceptor, a bacteriopheophytin) is at least two orders of magnitude faster than either the reduction of D^+ by cyt c^{2+} (or ferrocene) or the transfer of the electron from Q_A^- to Q_B. (ii) The state $DQ_A^-Q_B$ is in equilibrium with $DQ_AQ_B^-$ [16,30]. The partition coefficient α between these two states is defined by Eqn. 4a. After the second flash, the fraction of RCs in the state $DQ_AQ_B^-$ accepts a second electron to form $DQ_A^-Q_B^-$ and $DQ_AQ_B^{2-}$ (see iii). The inactive fraction in the state $DQ_A^-Q_B$ reequilibrates with $DQ_AQ_B^-$. (iii) $DQ_A^-Q_B^-$ is in equilibrium with $DQ_AQ_B^{2-}$ [31] (protonation omitted for simplicity). The partition coefficient β between these states is defined by Eqn. 4b. (iv) A *fraction* δ of RCs lack a bound Q_B. In this fraction DQ_A^- is formed after the first flash and is inactive after subsequent flashes. The distribution of states (Table A-I) based on i–iv is also discussed in Ref. 31. Note that if $[Q_B^{2-}]$ is taken to be the total concentration of all doubly-reduced (and protonated) Q_B, including any released from the RC, the table is valid whether or not excess exogenous quinone is present. With excess quinone present, doubly-reduced Q_B is displaced from the RC, which essentially reduces the concentration of $Q_A^-Q_B^-$ (and the value of the partition coefficient β) to zero.

Appendix B

Model for proton uptake kinetics

The proton uptake kinetics were modeled according to the scheme shown in Eqn. 16. The differential equations of the mol fractions, χ, of the different species are given by:

$$\frac{d\chi_{Q_A^-Q_B^-}}{dt} = -k_{AB}^{(2)} \cdot \chi_{Q_A^-Q_B^-} \tag{B-1a}$$

$$\frac{d\chi_{Q_A(Q_BH)^-}}{dt} = k_{AB}^{(2)} \cdot \chi_{Q_A^-Q_B^-} - k_{H^+(2)} \cdot \chi_{Q_A(Q_BH)^-} \tag{B-1b}$$

$$\chi_{Q_AQ_BH_2} = 1 - \chi_{Q_A^-Q_B^-} - \chi_{Q_A(Q_BH)^-} \tag{B-1c}$$

TABLE A-I

Distribution of reaction center and secondary donor species after successive laser flashes

Protonation has been omitted for simplicity. Fe^{2+} and Fe^{3+} represent the reduced and oxidized forms of the secondary electron donor, which in this work is either cytochrome *c* or ferrocene. Q_B^{2-} represents all the doubly-reduced Q_B, including any that has been released from the RC. The parameter δ is the fraction of RCs without a bound Q_B. The partition coefficients α between the states $Q_A^-Q_B$ and $Q_AQ_B^-$ and β between the states $Q_A^-Q_B^-$ and Q_B^{2-} are defined by Eqns. 4a and 4b, respectively. The assumptions for which the table is valid are discussed in the text.

Species number (i)	Species	Mol fraction (χ_i)		
		Before flashes	After one flash	After two flashes
1	Q_A	δ	0	0
2	Q_AQ_B	$1-\delta$	0	0
3	Fe^{2+} } ferrocene	n	$n-1$	$n-1-(1-\alpha)(1-\delta)$
4	Fe^{3+} } or cyt *c*	0	1	$1+(1-\alpha)(1-\delta)$
5	Q_A^-	0	δ	δ
6	$Q_A^-Q_B$	0	$\alpha(1-\delta)$	$\alpha^2(1-\delta)$
7	$Q_AQ_B^-$	0	$(1-\alpha)(1-\delta)$	$\alpha(1-\alpha)(1-\delta)$
8	$Q_A^-Q_B^-$	0	0	$\beta(1-\alpha)(1-\delta)$
9	Q_B^{2-}	0	0	$(1-\beta)(1-\alpha)(1-\delta)$

where for simplicity the proton concentration was assumed to be constant and the back reactions in Eqn. 16 were neglected. For the pH changes observed (< 0.05 units), the proton concentration was constant within 10%. Omission of the back reactions is justified at pH 7.5 and 21.5°C, since in both reactions the forward rate was found to be significantly larger than the reverse rate. For the first step in Eqn. 16, the equilibrium constant (i.e., ratio of forward to reverse rates) has been measured in mutant RCs (Glu-L212 → Gln) in which the second step is blocked; it was found to be approx. 10 at pH 7.5 and 21.5°C (Ref. 20 and McPherson et al., data not shown). Since Glu-L212 is believed to be protonated (i.e, electrically neutral like Gln) up to approx. pH 9.5 [19], the mutant and native RCs should exhibit the same kinetics at pH 7.5. For the second step in Eqn. 16, the equilibrium constant at pH 7.5 is approx. 10 (21.5°C) as indicated by the observed pK_a of approx. 8.5 for this step. [f]

The mol fractions of the three states as a function of time are obtained by solving Eqns. B-1 for the initial condition: $\chi_{Q_A^- Q_B^-} = 1$ at $t = 0$. The results are:

$$\chi_{Q_A^- Q_B^-} = e^{(-k_{AB}^{(2)} \cdot t)} \tag{B-2a}$$

$$\chi_{Q_A(Q_BH)^-} = \frac{k_{AB}^{(2)}}{\left(k_{H^+(2)} - k_{AB}^{(2)}\right)} \left(e^{(-k_{AB}^{(2)} \cdot t)} - e^{(-k_{H^+(2)} \cdot t)}\right) \tag{B-2b}$$

$$\chi_{Q_AQ_BH_2} = 1 - \left(1 + \frac{k_{AB}^{(2)}}{\left(k_{H^+(2)} - k_{AB}^{(2)}\right)}\right) e^{(-k_{AB}^{(2)} \cdot t)} + \left(\frac{k_{AB}^{(2)}}{\left(k_{H^+(2)} - k_{AB}^{(2)}\right)}\right) e^{(-k_{H^+(2)} \cdot t)} \tag{B-2c}$$

where it is assumed that the RCs are in one of the three states described by Eqns. B-2a–c, i.e., the sum of the three mol fractions is 1.0. The proton uptake after the second flash is given by:

$$H^+/RC = 1 \cdot \chi_{Q_A(Q_BH)^-} + 2 \cdot \chi_{Q_AQ_BH_2} \tag{B-3}$$

Eqn. 17 is obtained by substituting Eqns. B-2a–c into Eqn. B-3. Eqn. 17 predicts a steady-state uptake of 2.0 H^+/RC after the second flash; it has to be scaled to fit the observed H^+/RC, which is less than 2.0 (see Fig. 4b). The reasons why the observed proton uptake is less than 2.0 are: (i) Only a fraction $(1 - \alpha)(1 - \delta)$ of RCs form the two-electron states described by Eqns. B-2a–c; the remaining RCs are in a one-electron state (see Table A-I). (ii) D^+ is formed after the second flash and is present during the reaction shown in Eqn. 16 (see Results). The formation of D^+ causes a proton release (approx. 0.2 H^+/D^+ at pH 7.5) from amino-acid residues. (iii) The first and second steps in Eqn. 16 involve the removal of a negative charge from Q_A and Q_B, respectively. This causes a concomitant release of protons (negative pK_a shifts) from amino-acid residues that interact with the negative charges. The net, observed, proton uptake associated with the uptake of $H^+(1)$ or $H^+(2)$ will, therefore, be less than 1.0. Eqn. 17 will hold within an overall scale factor as long as the ratio of the proton uptake for the two steps in Eqn. 16 is 1:1. The 1:1 ratio is satisfied at pH 7.5 and 21.5°C as can be seen from the following: For the first step in Eqn. 16, the proton release from the residues is estimated to be the same as the proton release for the reaction $DQ_A^- \rightarrow DQ_A$, i.e., 0.31 H^+/Q_A^- at pH 7.5 (see Eqn. 11). For the second step, the proton release is estimated to be the same as the proton release for $DQ_AQ_B^- \rightarrow DQ_AQ_B$, i.e., 0.31 H^+/Q_B^- at pH 7.5 (see Eqn. 12). Therefore, the net observed proton uptake for each step in Eqn. 16 is the same, i.e., approx. 0.7 H^+/Q_B^{2-} and the 1:1 ratio holds.

[f] The equilibrium constant is defined by:

$$K_{eq} = \frac{[Q_AQ_BH_2]}{[Q_A(Q_BH)^-]} = 10^{(pK_a - pH)}$$

References

1 Feher, G. and Okamura, M.Y. (1978) in The Photosynthetic Bacteria (Clayton, R.K. and Sistrom, W.R., eds.), pp. 349–386, Plenum Press, New York.
2 Parson, W.W. (1987) in Photosynthesis (Amesz, J., ed.), pp. 43–61, Elsevier, New York.
3 Feher, G., Allen, J.P., Okamura, M.Y. and Rees, D.C. (1989) Nature 339, 111–116.
4 Dutton, P.L. (1986) in Encyclopedia of Plant Physiology, Vol. 19: Photosynthesis III (Staehelin, L.A. and Arntzen, C.J., eds.), pp. 197–237, Springer, New York.
5 Cramer, W.A. and Knaff, D.B. (1990) Energy Transduction in Biological Membranes, Springer-Verlag, New York.
6 Kirmaier, C. and Holten, D. (1987) Photosynth. Res. 13, 225–260.
7 Wraight, C.A. (1982) in Function of Quinones in Energy-Conserving Systems (Trumpower, B.L., ed.), pp. 181–197, Academic Press, New York.
8 Okamura, M.Y. and Feher, G. (1992) Annu. Rev. Biochem. 61, 861–896.
9 Wraight, C.A. and Stein, R.R. (1983) in The Oxygen Evolving System of Photosynthesis (Inoue, Y., Crofts, A.R., Govindjee, Murata, N., Renger, G. and Satoh, K., eds.), pp. 383–392, Academic Press, Japan.
10 McPherson, P.H., Okamura, M.Y. and Feher, G. (1990) Biochim. Biophys. Acta 1016, 289–292.
11 McPherson, P.H., Okamura, M.Y. and Feher, G. (1988) Biochim. Biophys. Acta 934, 348–368.
12 Clayton, R.K. and Straley, S.C. (1972) Biophys. J. 12, 1221–1234.
13 Slooten, L. (1972) Biochim. Biophys. Acta 275, 208–218.
14 Vermeglio, A. and Clayton, R.K. (1977) Biochim. Biophys. Acta 461, 159–165.
15 Feher, G., Okamura, M.Y. and McElroy, J.D. (1972) Biochim. Biophys. Acta 267, 222–226.
16 Wraight, C.A. (1979) Biochim. Biophys. Acta 548, 309–327.
17 Maroti, P. and Wraight, C.A. (1988) Biochim. Biophys. Acta 934, 314–328.

18 Maroti, P. and Wraight, C.A. (1988) Biochim. Biophys. Acta 934, 329–347.
19 Paddock, M.L., Rongey, S.H., Feher, G. and Okamura, M.Y. (1989) Proc. Natl. Acad. Sci. USA 86, 6602–6606.
20 Takahashi, E. and Wraight, C.A. (1992) Biochemistry 31, 855–866.
21 Takahashi, E. and Wraight, C.A. (1990) Biochim. Biophys. Acta 1020, 107–111.
22 Paddock, M.L., Rongey, S.H., McPherson, P.H., Feher, G. and Okamura, M.Y. (1991) Biophys. J. 59, 142a. (Abstract)
23 Paddock, M.L., Juth, A., Feher, G. and Okamura, M.Y. (1992) Biophys. J. 61, 153a. (Abstract)
24 Vermeglio, A. (1977) Biochim. Biophys. Acta 459, 516–524.
25 Maroti, P. and Wraight, C.A. (1990) Curr. Res. Photosynth. 1, 165–168.
26 Paddock, M.L., McPherson, P.H., Feher, G. and Okamura, M.Y. (1990) Proc. Natl. Acad. Sci. USA 87, 6803–6807.
27 Van Gelder, B.F. and Slater, E.C. (1962) Biochim. Biophys. Acta 58, 593–595.
28 Paddock, M.L., Rongey, S.H., Abresch, E.C., Feher, G. and Okamura, M.Y. (1988) Photosynth. Res. 17, 75–96.
29 Okamura, M.Y., Debus, R.J., Kleinfeld, D. and Feher, G. (1982) in Function of Quinones in Energy-Conserving Systems (Trumpower, B.L., ed.), pp. 299–317, Academic Press, New York.
30 Kleinfeld, D., Okamura, M.Y. and Feher, G. (1984) Biochim. Biophys. Acta 766, 126–140.
31 Kleinfeld, D., Okamura, M.Y. and Feher, G. (1985) Biochim. Biophys. Acta 809, 291–310.
32 Straley, S.C., Parson, W.W., Mauzerall, D.C. and Clayton, R.K. (1973) Biochim. Biophys. Acta 305, 597–609.
33 Morrison, L.E., Schelhorn, J.E., Cotton, T.M., Bering, C.L. and Loach, P.A. (1982) in Function of Quinones in Energy-Conserving Systems (Trumpower, B.L., ed.), pp. 35–58, Academic Press, New York.
34 Maroti, P. and Wraight, C.A. (1989) Biophys. J. 55, 428a. (Abstract)
35 Diner, B.A., Schenck, C.C. and De Vitry, C., (1984) Biochim. Biophys. Acta 766, 9–20.
36 Okamura, M.Y., Isaacson, R.A. and Feher, G. (1975) Proc. Natl. Acad. Sci. USA 72, 3491–3495.
37 Rongey, S.H., Paddock, M.L., Juth, A.L., McPherson, P.H., Feher, G. and Okamura, M.Y. (1991) Biophys. J. 59, 142a. (Abstract)
38 McPherson, P.H., Schönfeld, M., Paddock, M.L., Feher, G. and Okamura, M.Y. (1990) Biophys. J. 57, 404a. (Abstract)
39 McPherson, P.H., Paddock, M.L, Okamura, M.Y. and Feher, G. (1993) Biophys. J. 64, 18a. (Abstract)
40 Allen, J.P., Feher, G., Yeates, T.O., Komiya, H. and Rees, D.C. (1988) Proc. Natl. Acad. Sci. USA 85, 8487–8491.
41 Harrowfield, J.M., Norris, V. and Sargeson, A.M. (1976) J. Am. Chem. Soc. 98, 7282–7289.
42 Bauscher, M., Nabedryk, E., Bagley, K., Breton, J. and Mantele, W. (1990) FEBS Lett. 261, 191–195.
43 Braiman, M.S., Tatsushi, M., Marti, T., Stern, L.J., Khorana, H.G. and Rothschild, K.J. (1988) Biochemistry 27, 8516–8520.